

# Demonstration of MEMS-Controlled Electronic States in Single Quantum Dots

T. Nakaoka<sup>1</sup>, T. Kakitsuka<sup>2</sup>, T. Saito<sup>1</sup>, and Y. Arakawa<sup>1,2</sup>

<sup>1</sup> RCAST, IIS, and CCR, University of Tokyo, 4-6-1, Komaba, Meguro-ku, Tokyo 153-8505, Japan  
Phone: +81-3-5452-6098-57590, FAX: +81-3-5252-6247, Email: nakaoka@iis.u-tokyo.ac.jp

<sup>2</sup> NTT Photonics Laboratories, NTT Corporation, 3-1 Morinosato Wakamiya, Atsugi, Kanagawa 243-0198, Japan

## 1. Introduction

Quantum dots (QDs) have attracted considerable interest because their atomlike properties make them a good venue for studying the physics of confined carriers and for realization of advanced photonic and electron devices [1,2]. Quantum mechanical control of the electronic states of QDs allows one to manipulate single electrons and single photons, which leads to novel device applications in fields such as quantum cryptography, quantum computing, optics, and optoelectronics [3,4]. Such fine control of the electronic states has been generally done by external current, voltage, or magnetic fields.

In this work, we control the energy levels of single quantum dots via strain by embedding the dots into a micromachined airbridge. To our knowledge, this is the first use of microelectromechanical systems (MEMS) technology in controlling three-dimensionally quantum-confined states. The deformation of the airbridge by an electrostatic voltage induces strain distribution in the bridge. The strain modifies the electronic states of the QDs because the dots are strained coherently with the surrounding matrix [5]. The energy level shift of the QDs due to the bridge deformation is monitored by micro-photoluminescence (PL) measurement. The effect of the strain on the electronic states is evaluated with the aid of theoretical calculation using a finite element method.

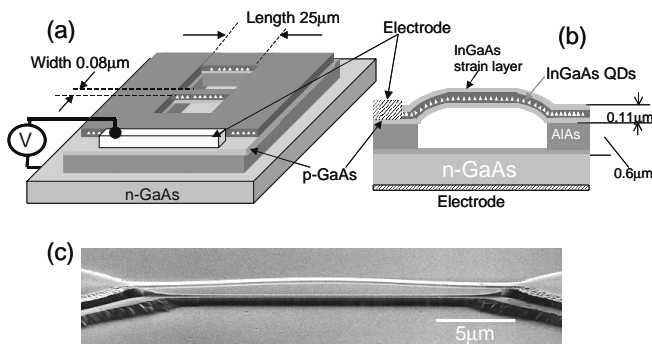


Fig. 1 (a) Schematic illustration of MEMS structure. (b) Cross-sectional view of the airbridge. (c) SEM picture of the airbridge

## 2. Experiments

The self-assembled InGaAs QDs were grown at 500°C and 76 Torr on an n-doped GaAs (100) wafer by metal organic chemical vapor deposition. Atomic force microscopy measurement of a reference uncapped sample reveals the average QD diameter of 20 nm and height of 7 nm, as well as the areal density of about  $1 \times 10^{10}$  /cm. The sample structure consists of a thin GaAs buffer layer, followed by a AlAs sacrificial layer, a p-doped GaAs layer

and an InGaAs dot layer embedded in GaAs layers covered by a 7 nm thick  $\text{In}_{0.2}\text{Ga}_{0.8}\text{As}$  strain layer. The samples were laterally patterned by electron beam lithography and reactive ion etching techniques. The patterned structure is shown in Fig. 1(a) and (b). An airgap was formed by removal of the AlAs sacrificial layer using buffered HF solution [6,7,8]. After the removal, the samples were dried using a  $\text{CO}_2$  critical point drying technique. The airbridge shows a slightly bowed shape [Fig. 1(c)] due to the relaxation of the misfit strain between the GaAs layer and the InGaAs strain layer [5,9]. The introduction of the InGaAs strain layer and the critical drying technique serve to prevent the structure from sticking.

The fabricated airbridge is 25  $\mu\text{m}$  long, 0.8  $\mu\text{m}$  wide, and 0.11  $\mu\text{m}$  high. The base of the QDs lies at a height of 80 nm from the bottom of the bridge. When a reverse bias voltage is applied between the p-doped GaAs layer and the n-doped substrate, an electrostatic force pulls the airbridge down. By this downward deformation, additional compressive strain is applied on the dots embedded near the top of the bridge. In the MEMS structure, the electric field should not be applied directly to the QDs since the p-doped layer exists below the QD layer.

Micro-PL measurement of the QDs was performed at 3.6 K in a continuous-flow  $^4\text{He}$  cryostat. The PL was excited with the 632.8 nm line of a He-Ne laser beam focused by a microscope objective to a diameter of about 2  $\mu\text{m}$ . The excitation power density is about 50  $\text{W}/\text{cm}^2$ . The PL was collected by the objective, dispersed by a triple grating monochromator, and detected by a liquid  $\text{N}_2$  cooled Si charge-coupled device (CCD) camera.

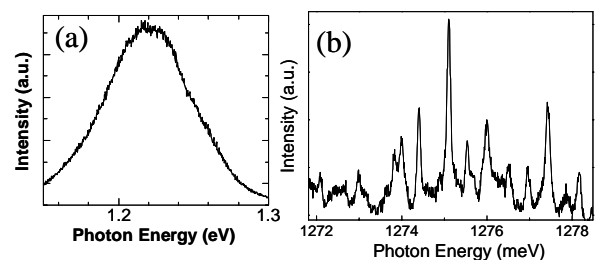


Fig. 2 (a) Macro-PL spectrum of the as-grown QDs. (b) Micro-PL spectrum of the QDs in the airbridge.

## 3. Results and Discussion

While the macro-PL spectrum [Fig. 2(a)] exhibits a inhomogeneously broadened line shape, the micro-PL spectrum [Fig. 2(b)] in the micromachined airbridge with a width of 0.8  $\mu\text{m}$  resolves separate emissions from hundreds of individual QDs. The peaks are assigned to the ground

state emissions because these peaks are not saturated at the excitation power density.

Figure 3(a) shows the expanded views of the micro-PL spectra in the micromachined airbridge. The variation of the peak energy is plotted in Fig. 3(b) as a function of time. When a reverse voltage of 5.5 V is applied, the peak shows a blue shift. The blue shift is attributed to the additional compressive strain due to the bridge deformation because such a PL peak shift is not observed in the sample regions other than the airbridge. It should be noted that other possible effects such as heating and stark effect [8,10] should induce a red shift. When the bias voltage is reset to 0 V, the peak shows a redshift, but does not return to the initial value. This will be due to some plastic irreversible deformation. In the second and the following cycles of the bias voltage application, the switching is nearly reversible.

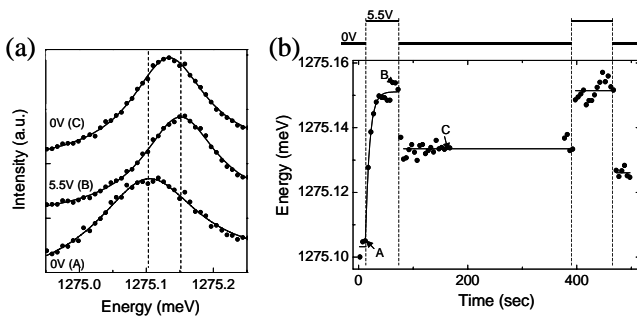


Fig. 3 (a) Micro-photoluminescence spectra of the QDs in the airbridge for several bias voltages. The spectral line shapes are fitted by Lorentzians. (b) PL peak energy plotted versus time. The bias voltage variation is shown above. The labels A, B, and C correspond to those in (a).

In order to evaluate the strain effect quantitatively, we calculate the strain induced by the bridge deformation and the following energy shift. First, we estimate the deformation of the bridge under applied bias voltage by the one-dimensional Karman equation [11]. Then, the strain distribution in the deformed bridge is calculated by a finite element calculation under applied uniform loads to reproduce the deformed shape. The strain distribution around the QD is obtained by applying the strain in the bridge as the boundary condition on the small box modeling the QD vicinity. Finally, the energy level shift following the shape change is calculated by solving three-dimensional Schrödinger equation taking into account the strain distribution around the QD embedded in the bridge. The details on the calculation procedure is described elsewhere [5].

Figure 4 shows the calculated energy shift which agrees well with the experimental energy shift due to the elastic deformation. The calculation demonstrates that the observed energy shift is due to the strain variation induced by the bridge deformation. It is noteworthy that the calculation shows strain-induced modifications of not only the energy levels of the QDs but also the wave functions.

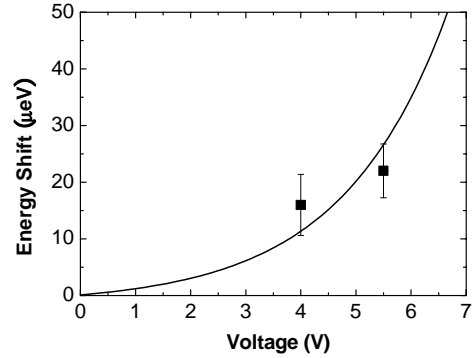


Fig. 4 Calculated energy shift (solid line) and the experimental one (solid square) for second voltage application, plotted as a function of the bias voltage. The error bar is based on the standard deviation of the measurements.

### 3. Conclusions

We have demonstrated that the energy levels of the single QDs can be controlled by using the MEMS structure. The energy shift of single QDs is observed by micro-PL measurement applying the reverse bias voltage on the MEMS structure. We have evaluated the deformation-induced energy shift quantitatively by the calculation which agrees well with the experiment. This work suggests a new approach to finely control the electronic states of the single QDs without charging effects.

### Acknowledgements

This work was supported in part by the IT program (RR2002) from the Ministry of Education, Science, Sports, and Culture, and also by Grant-in-Aid for COE Research (#12CE2004 “Control of Electrons by Quantum Dot Structures and Its Application to Advanced Electronics”).

### References

- [1] Y. Arakawa and H. Sakaki, *Appl. Phys. Lett.* 40 (1982) 939.
- [2] D. Bimberg, M. Grundmann, and N. N. Ledentsov, *Quantum Dot Heterostructures* (John Wiley & Sons Ltd., New York, 1999).
- [3] C. Santori *et al.*, *Phys. Rev. Lett.*, 86 (2001) 1502.
- [4] P. Michler *et al.*, *Science* 290 (2000) 2282.
- [5] T. Nakaoka *et al.*, *Phys. Rev. B*, submitted.
- [6] T. Nakaoka *et al.*, *Appl. Phys. Lett.*, 81 (2002) 3954.
- [7] H. Yamaguchi, R. Dreyfus, and Y. Hirayama, *Appl. Phys. Lett.* 78 (2001) 2372.
- [8] I. E. Itskevich *et al.*, *Appl. Phys. Lett.* 76 (2000) 3932.
- [9] P. O. Vaccaro, K. Kubota, and T. Aida, *Appl. Phys. Lett.* 78 (2001) 2852.
- [10] P.W. Fry *et al.*, *Phys. Rev. Lett.* 84 (2000) 733.
- [11] P.M. Osterberg and S.D. Senturia, *J. Microelectromech. syst.* 6 (1997) 107.